

Analysis and Design of Large Array Antennas Using a Fast Direct Solver

Min Zhou¹, Martin H. Gæde¹, Søren Hartmann¹, Pasquale G. Nicolaci¹, Michael F. Palvig¹, Niels Vesterdal¹,
Magnus Brandt-Møller¹, Asger Limkilde¹, Edorardo Baldazzi¹, Erik Jørgensen¹, Giovanni Toso²

¹TICRA, Copenhagen, Denmark, mz@ticra.com

²European Space Agency (ESA-ESTEC), Noordwijk, The Netherlands, giovanni.toso@esa.int

Abstract—This paper presents the application of TICRA’s recent full-wave analysis advancements for antenna arrays, with a particular emphasis on the use of the Fast Direct Solver (FDS). We showcase the effectiveness of this method through real-world examples, including a 10×10 spline horn array, a 218 circular horn array, and a 25×25 microstrip patch array. The results demonstrate that the FDS-based approach offers significant improvements in efficiency and memory usage compared to traditional methods.

I. INTRODUCTION

In the new era of satellite constellations such as Starlink, and with a quest for flat-panel portable user terminals, flexible satellite payloads, 6G wireless communications, and advanced radar systems, phased-array antennas are ubiquitous. For larger flexibility and to ensure low-power and stable communication links, electrically large antenna arrays are required. Their performance is nevertheless contingent upon accurately predicting antenna array performance through rigorous methods based on computational electromagnetics. Due to the electrical size of such arrays, full-wave simulations of electrically large arrays are not possible with existing commercial tools. Therefore, one resorts to designing large arrays using the infinite array assumption or other approximations. These methods lead to sub-optimal performance since the active reflection coefficients of the individual array elements cannot be predicted when the beamforming coefficients are optimized, due to the lack of an accurate model of the mutual coupling between array elements. Therefore, mutual coupling is generally considered a parasitic effect that should be avoided. If a more accurate analysis approach is applied, all coupling effects are included when optimizing beamforming coefficients and the active reflection coefficients of the individual array elements can be constrained to the permissible range. In this case mutual coupling is included as an inherent property of the array, which can be exploited instead of being avoided.

Full-wave methods such as Method of Moments (MoM) [1] and Multi-Level Fast Multipole Method (MLFMM) [2] do not take advantage of the repetitive nature of arrays, resulting in substantial computational demands for large arrays. To address this, specialized full-wave method based on the Array Decomposition Method (ADM) [3], [4] can be considered, enabling full-wave simulations of complex antenna arrays with thousands of elements to be completed in just a few minutes on a laptop. While ADM has proven to be exceptional

efficient, a key limitation is that ADM relies on the use of iterative algorithms. As a consequence, the full analysis must be repeated for each excitation to compute the complete scattering matrix of the array. This can result in prolonged simulation times for arrays with numerous excitations. This issue is circumvented using a Fast Direct Solver (FDS) algorithm [5] that uses fast direct matrix factorization of a highly compressed system matrix [6], [7]. This approach mitigates the problem of multiple excitations (right-hand sides, RHS) and provides the full scattering matrix of the array in roughly the same time as a single excitation. This allows all coupling effects to be rigorously included in the design phase, even for arrays with several thousand elements.

The development presented in [5] was only applied for all-metallic structures. In this paper, we show how the FDS can also be applied to handle dielectric structures. Furthermore, as part of the development of a specialized design and analysis software tool for array antennas, the FDS algorithm has been implemented within the TICRA Tools [8] framework. This integration ensures that these advancements are seamlessly integrated in TICRA Tools, allowing us to leverage all the software’s capabilities. The results shared reflect the current state of the development at the time of writing. As the algorithms continue to evolve and improve, more up-to-date results will be provided at the conference.

II. FAST DIRECT SOLVER

Fast Direct Solver (FDS) is a method that solves the MoM equations by approximating a factorization of the system matrix, thus allowing for efficient solutions to multiple RHS. Once the factorization is computed, subsequent solves become much faster, making them well-suited for problems with many excitations, e.g., array antennas.

Hierarchical matrices [6] have emerged as a core framework of fast direct solvers, offering data-sparse representations that reduce both time and memory requirements, while offering the ability to efficiently compute factorizations [7], [9]. The FDS implementation by TICRA is focused on \mathcal{H}^2 -matrices [10], which is a specialized type of hierarchical matrices which offers a flexible framework and comes with powerful asymptotic scaling in both time and memory. Furthermore, the FDS implementation adapts the use of higher-order basis functions from [11], which provides significant reductions

in both computational time and memory requirements. The following section provides a brief overview of the FDS.

A \mathcal{H}^2 matrix is used to efficiently represent the MoM matrix \mathbf{Z} . This matrix format exploits the block low-rank structure resulting from the singular Helmholtz kernel. To express the block low-rank structure, a cluster tree is used to recursively partition the domain of unknowns into clusters of constant size. A \mathcal{H}^2 matrix compresses entire block rows and columns, such that the block between clusters s and t is represented as:

$$\mathbf{Z}_{st} \simeq \mathbf{Q}_s \mathbf{B}_{st} \mathbf{V}_t^H. \quad (1)$$

We compute the orthogonal bases of rows and columns in (1) by utilizing randomized linear algebra and MLFMM, which approximates matrix-vector products as

$$\mathbf{Z}\mathbf{v} \simeq \mathbf{Z}_{\text{near}}\mathbf{v} + \mathbf{Z}_{\text{far}}\mathbf{v}, \quad (2)$$

where \mathbf{Z}_{near} is sparse and \mathbf{Z}_{far} can be applied efficiently in $\mathcal{O}(N \log N)$ time. The orthonormal row and column bases \mathbf{Q} and \mathbf{V} are computed as the range of the sketch:

$$\mathbf{Y} = \mathbf{Z}_{\text{far}}\mathbf{\Omega}, \quad \mathbf{X} = \mathbf{Z}_{\text{far}}^H\mathbf{\Psi}, \quad (3)$$

where $\mathbf{\Omega}, \mathbf{\Psi} \in \mathbb{R}^{N \times r}$ and the entries are i.i.d. normal distributed [12]. Products with \mathbf{Z}_{far} allows for sketching of all rows/columns simultaneously, and the sketching is repeated for each level in a bottom-up fashion. Sketching of the entire matrix requires $\mathcal{O}(r \log N)$ matrix-vector products in total.

A common strategy for factorizing \mathcal{H}^2 matrices aims at finding a transformation such that the problem implicitly becomes a sparse factorization problem [9]. The used factorization utilizes that all coupling matrices \mathbf{B}_{st} are orthogonal to the nullspace of the row and column bases $\mathbf{Q}_s, \mathbf{V}_t$

$$\begin{pmatrix} \mathbf{Q}_s & \mathbf{Q}_s^\perp \end{pmatrix}^H \mathbf{Q}_s \mathbf{B}_{st} \mathbf{V}_t^H \begin{pmatrix} \mathbf{V}_t & \mathbf{V}_t^\perp \end{pmatrix} = \begin{pmatrix} \mathbf{B}_{st} & \mathbf{0} \\ \mathbf{0} & \mathbf{0} \end{pmatrix}, \quad (4)$$

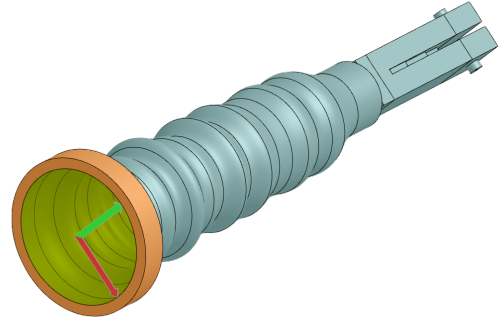
thus allowing for efficient elimination of all sparsified indices. This is then repeated for each group in each level, until we are left with a small dense matrix which needs to be factorized.

III. APPLICATION EXAMPLES

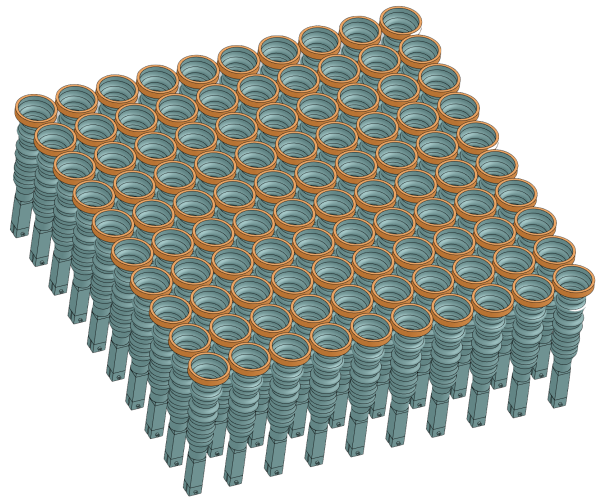
A. Spline Horn Array I

The first example demonstrating the capabilities of the FDS is a 10×10 spline horn array operating at 20 GHz, see Fig 1. The individual horn, shown in Fig 1a, features a septum polarizer connected to the horn interior via a rectangular-to-circular waveguide transition, with the interior defined by an optimized spline profile. The horn exterior is a short section of circular waveguide attached to the spline profile's end. While this horn can be analyzed using MoM/MLFMM, CHAMP 3D [13] allows mode-matching to solve the horn's interior in just a few seconds.

Since our FDS implementation is fully integrated with TICRA Tools, including CHAMP 3D, we can combine methods to efficiently account for mutual coupling between feed horns. In Fig 1b, we show an array of feed horns. The horn interior results, solved using CHAMP 3D, are reused across



(a)



(b)

Fig. 1: 10×10 spline horn array, a) individual horn geometry including septum polarizer and waveguide transitions, b) full horn array.

the array, while the coupling between horns, governed by their exteriors, is handled using FDS. This approach enables the full analysis of the horn array within minutes.

This configuration results in a problem with 4200 RHS. If an iterative solver like MLFMM were used, the problem would need to be solved 4200 times, resulting a total simulation time more than 24 hours. Due to the size of the horn array and the use of CHAMP 3D for the horn interiors, the problem can be efficiently analyzed using the HO-MoM (direct factorization method) in ESTEAM, which will serve as the reference solution for this case. In addition to the radiation pattern, we also calculate the full scattering matrix of the array.

In Fig. 2 both the radiation pattern of the horn array computed by HO-FDS and HO-MoM are shown. It is seen that there is a perfect agreement between HO-FDS and HO-MoM.

Table I compares the performance of the HO-FDS and HO-MoM. For HO-MoM the solution time is around half a

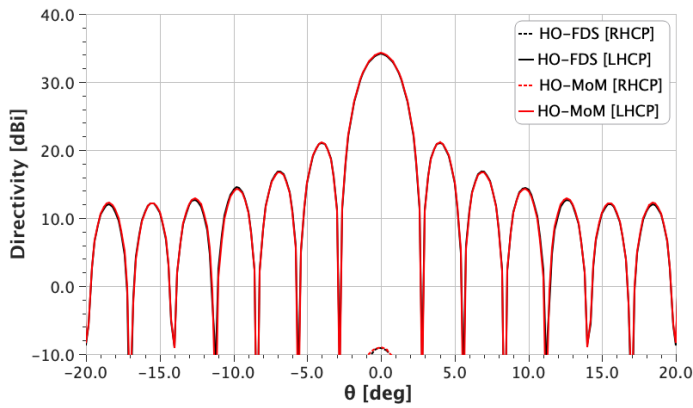


Fig. 2: Far-field directivity pattern at 20 GHz of spline horn array.

hour and requires a memory consumption of 54 GB. For HO-FDS, this is greatly reduced to a solution time of 6 minutes and only 10 GB of memory. In terms of memory, the use of MLFMM may reduce the required memory consumption. However, given the number of RHS, MLFMM is not by no means competitive in terms of simulation time.

In this test case, if CHAMP 3D were not used to analyze the horn interior and the entire horn array were analyzed solely with HO-MoM, the required memory consumption would make this unfeasible. However, with the system matrix compression, this is still achievable using HO-FDS.

B. Spline Horn Array II

Because of the low memory consumption needed to carry out the simulation of the horn array using HO-FDS and CHAMP 3D, we consider here a bigger horn case consisting of different horn sizes. The configuration is shown in Fig. 3. The array is based on the active lens antenna concept presented in [14] and constitutes the front array of a similar discrete lens antenna.

The array consists of 218 spline horns arranged in concentric rings. The spline horns aperture sizes have been optimized to implement the density taper on the array aperture. In fact, the feeds are fed with the same level of signal, but the different sizes of the apertures entail a different power density which means an amplitude taper at the array aperture. This is clearly

TABLE I: Simulation time and memory consumption for 10×10 spline horn array on an Intel Core i7-13850HX 2.1GHz with 20 cores laptop.

Method	Total Simulation Time	Memory Consumption
HO-MoM + CHAMP 3D	30 min	54 GB
HO-FDS + CHAMP 3D	6 min	10 GB

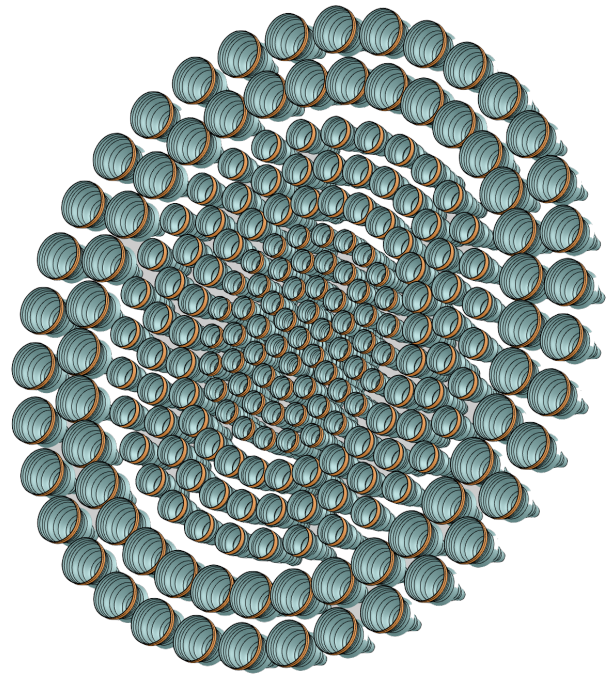


Fig. 3: Circular horn array.

showed in Fig. 4 where the inner rings have high power, and the external rings have lower power. This tapering was achieved using only four different feed aperture sizes. This configuration results in a problem with 4360 RHS.

The radiation pattern of the horn array is shown in Fig. 5 and the Table II summarizes the performance of the HO-FDS.

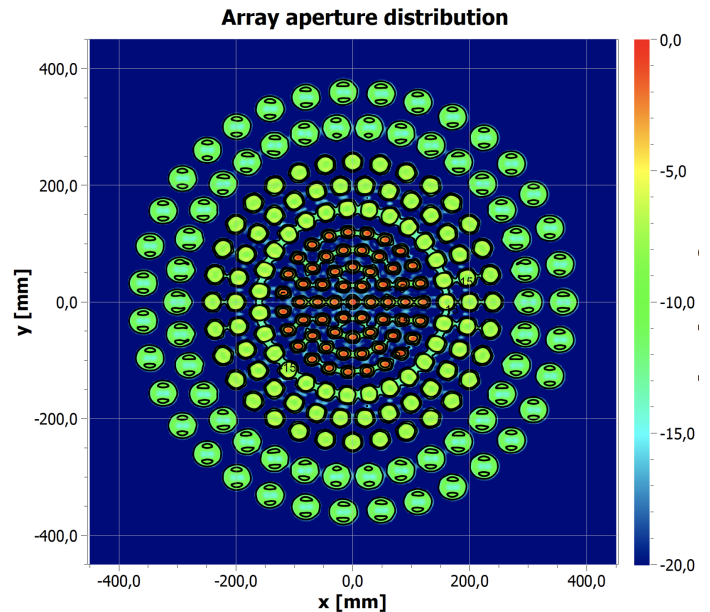


Fig. 4: Array aperture near-field field distribution.

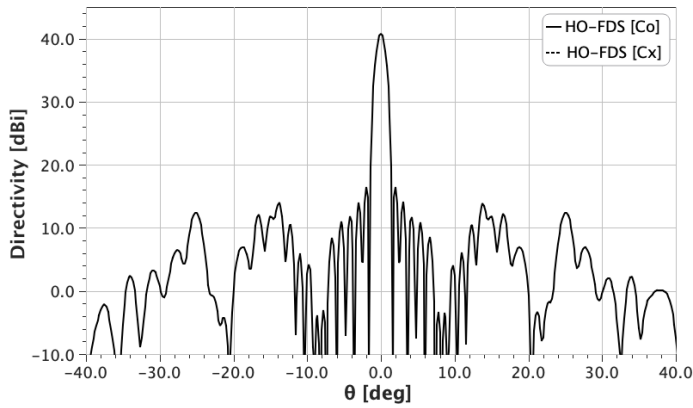


Fig. 5: Far-field directivity pattern at 19.5 GHz of circular horn array.

TABLE II: Simulation time and memory consumption for circular spline horn array on an AMD Ryzen 9 5950X machine with 16 cores.

Method	Total Simulation Time	Memory Consumption
HO-FDS + CHAMP 3D	14 min	25 GB

C. Microstrip Patch Array

The application examples shown up until now all consists of all-metallic structures. To demonstrate the capabilities of handling dielectric structures, we consider here a 25×25 microstrip patch array. The array is shown in Fig. 6 as well as the employed simulation mesh. The patch array operates at 30 GHz and consists of a rectangular patch element printed on a single layer dielectric substrate with $\epsilon_r = 2.2$ and $\tan\delta = 0.0009$. To facilitate circular polarization, each patch element is fed by two coaxial ports in phase quadrature and 5 modes were required on each port to obtain an accurate computation of the scattering matrix of the full array. This configuration leads to a problem with 6250 RHS.

Due to the large electrical size, HO-MoM is not a viable option. Similarly, the number of RHS makes HO-MLFMM impractical due to the excessive simulation time required. By utilizing HO-FDS, the problem, including the computation of the array's scattering parameters and radiation pattern, can be solved in 2 hours with a current memory requirement of 100 GB, see Table III. The radiation pattern of the array is shown Fig. 7.

The current FDS implementation is still work in progress and has not yet been optimized for either memory usage or speed. Several steps can be taken to enhance FDS performance. For example, the symmetry properties of the linear equations are not currently leveraged, and the array's repetition characteristics are also not exploited, both of which could lower computational requirements. Once these improvements are implemented and the algorithm is fully optimized, we

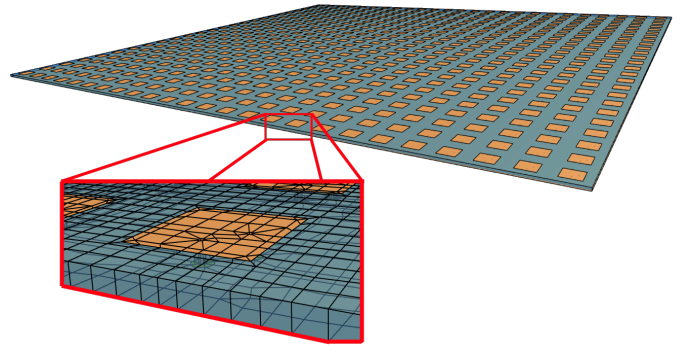


Fig. 6: 25×25 -element microstrip patch array.

TABLE III: Simulation time and memory consumption for 25×25 patch array on a Xeon E5-2690 v3 2.6 GHz with 12 cores workstation.

Method	Total Simulation Time	Memory Consumption
HO-FDS	2 hours	100 GB

expect that this patch array will require only 50 GB of memory and can be simulated in approximately 1 hour.

IV. CONCLUSIONS

This paper presents TICRA's recent advancements in full-wave analysis methods for antenna arrays, focusing on the Fast Direct Solver (FDS). These developments offer improved efficiency in solving complex electromagnetic problems for large arrays.

We demonstrate the FDS method on real-world examples, including a 10×10 spline horn array, a 218-element circular horn array, and a 25×25 microstrip patch array. Results show that the FDS outperforms traditional methods in efficiency and memory consumption, significantly reducing simulation times. This speed enables the practical optimization of finite arrays, making iterative design processes more feasible and efficient.

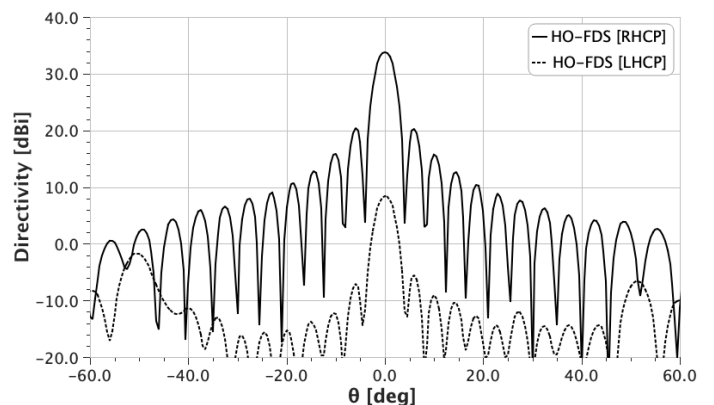


Fig. 7: Far-field directivity pattern at 30 GHz of microstrip patch array.

REFERENCES

- [1] R. Harrington, *Field computation by moment methods*. Macmillan, 1968.
- [2] J. M. Song and W. C. Chew, "Multilevel fast-multipole algorithm for solving combined field integral equations of electromagnetic scattering," *Microwave and Optical Technology Letters*, vol. 10, no. 1, pp. 14–19, Sep. 1995.
- [3] M. Brandt-Møller, M. Mattes, O. Breinbjerg, M. Zhou, and E. Jørgensen, "Higher-order array decomposition method for array antennas with connected elements," in *2023 IEEE International Symposium on Antennas and Propagation and USNC-URSI Radio Science Meeting (USNC-URSI)*. IEEE, 2023, pp. 585–586.
- [4] —, "Extended higher-order array decomposition method for fully populated or thinned array antennas and scatterers with connected elements," *IEEE Trans. Antennas Propag.*, vol. 72, no. 5, pp. 4454–4464, 2024.
- [5] M. H. Gæde, M. S. Andersen, A. Limkilde, O. Borries, and J. S. Hesthaven, "A fast direct solver for higher order discretizations of integral equations," in *2024 IEEE International Symposium on Antennas and Propagation and USNC-URSI Radio Science Meeting (USNC-URSI)*. IEEE, 2024.
- [6] W. Hackbusch, "Sparse matrix arithmetic based on H-matrices. Part I: Introduction to H-matrices," *Computing (vienna/new York)*, vol. 62, no. 2, pp. 89–108, 1999, publisher: Springer-Verlag Wien.
- [7] —, *Hierarchical matrices: Algorithms and analysis*. Springer, 2015.
- [8] "TICRA Tools," <https://www.ticra.com/software/all-software/>.
- [9] M. Ma and D. Jiao, "Accuracy directly controlled fast direct solution of general H₂-matrices and its application to solving electrodynamic volume integral equations," *EEE Trans. Microw. Theory Techn.*, vol. 66, no. 1, pp. 35–48, 2018.
- [10] Hackbusch, W. and Khoromskij, B. and Sauter, S. A., "On H₂-matrices," in *Lectures on Applied Mathematics*, H.-J. Bungartz, R. H. W. Hoppe, and C. Zenger, Eds. Berlin, Heidelberg: Springer, 2000, pp. 9–29.
- [11] E. Jørgensen, J. L. Volakis, P. Meincke, and O. Breinbjerg, "Higher order hierarchical legendre basis functions for electromagnetic modeling," *IEEE Trans. Antennas Propag.*, vol. 52, no. 11, pp. 2985–2995, 2004.
- [12] N. Halko, P. G. Martinsson, and J. A. Tropp, "Finding structure with randomness: Probabilistic algorithms for constructing approximate matrix decompositions," *SIAM Review*, vol. 53, no. 2, pp. 217–288, 2011.
- [13] "CHAMP3D," <https://www.ticra.com/software/champ3d/>.
- [14] G. Ruggerini, P. G. Nicolaci, G. Toso, and P. Angeletti, "A Ka-band active aperiodic constrained lens antenna for multibeam applications," *IEEE Antennas and Propagation Magazine*, vol. 61, no. 5, pp. 60–68, 2019.